World Journal of Advanced Research and Reviews
eISSN: 2581-9615 CODEN (USA): WJARAI
Cross Ref DOI: 10.30574/wjarr
Journal homepage: https://wjarr.com/

(RESEARCH ARTICLE)

PETROGRAPHIC CHARACTERIZATION OF GOLD-BEARING QUARTZ VEINS MINED BY ARTISANAL OPERATIONS IN THE DOROPO REGION, BOUNA, NORTHEASTERN CÔTE D'IVOIRE: IMPLICATIONS FOR GOLD MINERALIZATION

Aboubakar Sidik OUATTARA [1,*], Inza COULIBALY [1], Akissi Bienve Pélagie KOUAKOU [1], Yacouba Droh Lanciné COULIBALY [2] and GONE [1]

[1] Nangui ABROGOUA University, UFR of Environmental Sciences and Management, Geosciences and Environment Laboratory, 02 BP 801 Abidjan 02, Côte d'Ivoire.
[2] Félix HOUPHOUET-BOIGNY University, UFR of Earth Sciences and Mineral Resources, Laboratory of Geology, Mineral and Energy Resources, 22 BP 582 Abidjan 22, Côte d'Ivoire.
* Corresponding Author

World Journal of Advanced Research and Reviews, 2026, 32(02), 605–615

Publication history: Received on 27 September 2026; revised on 03 November 2026; accepted on 05 November 2026

Article DOI: https://doi.org/10.30574/wjarr.2026.32.2.2798

Copyright © 2026 Author(s) retain the copyright of this article. This article is published under the terms of the Creative Commons Attribution License 4.0

ABSTRACT

The Doropo region, located in northeastern Côte d'Ivoire within the Paleoproterozoic Birimian terranes of the West African Craton, represents a key sector marked by a major intensification of artisanal gold mining activities. This study provides a detailed petrographic and structural characterization of gold-bearing quartz veins to clarify their emplacement mechanisms and metallogenic implications. Field investigations combined with petrographic analyses identified three main quartz morphotypes: (i) milky quartz, (ii) smoky quartz, and (iii) saccharoidal quartz. These veins are preferentially hosted within NNE–SSW to NE–SW trending ductile-brittle shear zones, locally crosscut by late NW–SE fractures. The observed microstructures (undulatory extinction, dynamic recrystallization, subgrain development, sub-microfracturing) reflect syn- to post-crystalline deformation associated with Eburnean orogenic phases. The opaque mineral assemblage consists of pyrite, arsenopyrite, chalcopyrite, and secondary iron oxide phases. Smoky quartz shows the highest correlation with high gold grades due to the combined presence of sulfide inclusions and a dense microfracture network favoring the trapping of mineralizing hydrothermal fluids. Saccharoidal quartz results from intense dynamic recrystallization (granulation), whereas milky quartz corresponds to the early episodes of the siliceous system. Overall, these attributes confirm that the Doropo district fits the model of syn-tectonic mesothermal orogenic gold deposits controlled by Birimian crustal strike-slip faults.

Keywords: Birimian; Orogenic; Hydrothermal alteration; Doropo; Côte d'Ivoire.

1 INTRODUCTION

The Paleoproterozoic domain of the West African Craton (WAC), more commonly referred to as the Birimian province, represents one of the most fertile gold metallogenic districts on the planet (Milési *et al.*, 2004; Groves *et al.*, 2018). Formed mainly between 2.25 and 2.00 Ga during the Eburnean orogeny, this craton consists of volcano-sedimentary

greenstone belts separated by vast sedimentary basins and intruded by several generations of granitic and granodioritic complexes (Bessoles, 1977; Vidal and Alric, 1994; Block *et al*., 2016). The gold mineralizations spatially associated with these terranes are overwhelmingly controlled by large-scale crustal shear corridors developed during the Eburnean compressional and transcurrent phases (Goldfarb *et al*., 2001, 2005; Feybesse *et al*., 2006; Baratoux et al., 2011).

In this regional context, gold-bearing hydrothermal systems are generally expressed as networks of quartz-carbonate veins hosted within zones of intense deformation. Gold precipitation is accompanied by pervasive wall-rock hydrothermal alteration marked by sericitization, carbonatization, silicification, and sulfidation of the host rocks (Groves *et al*., 2003; Goldfarb and Groves, 2015; Goldfarb *et al*., 2020). The mineralizing fluids, preferentially of metamorphic origin, migrate through structurally permeable networks under intermittent fluid-pressure regimes (Robert and Poulsen, 2001; Groves and Goldfarb, 2018).

Côte d'Ivoire occupies a central position within the southern Birimian domain (Baoulé-Mossi domain) (Kouamelan *et al*., 2015; Yao e*t al*., 2016). The Doropo sector, located in the far northeast of the country near the border with Burkina Faso, has experienced in recent years a dramatic rise in artisanal gold mining. Despite this intense artisanal mining activity and the recent discovery of significant resources by exploration companies (Siagné *et al*., 2022), detailed petrographic and microstructural studies of the vein structures underlying these gold concentrations remain fragmentary.

The study of quartz textures, its deformation microstructures, and the characterization of associated sulfide phases nonetheless constitutes a first-order tool for reconstructing the deformation history, the hydrothermal fluid-circulation regime, and the mechanisms of mineralization deposition (Lawrence *et al*., 2013; Allibone *et al*., 2002).

The main objective of this study is to establish a detailed petrographic typology of the various categories of quartz veins mined in the Doropo region, while analyzing their deformation microstructures and associated sulfide assemblages, in order to assess the degree of affiliation of this system with the classic models of Birimian orogenic gold deposits and to guide future targeted exploration campaigns in northeastern Côte d'Ivoire.

2 REGIONAL AND LOCAL GEOLOGICAL SETTING

The study area, included in the Doropo region, is bounded by coordinates 3°17' and 3°11' longitude and 9°44' and 9°45' latitude. The Doropo region, located in northeastern Côte d'Ivoire, lies 76.6 km from Bouna and approximately 648.6 km from Abidjan. The regional geological framework belongs to the Léo-Man shield. The Baoulé-Mossi domain is characterized by an arrangement of volcano-sedimentary units aligned N–S to NE–SW **(figure 1 A).** The layered assemblages comprise tholeiitic lavas (basalts, andesites), pyroclastic rocks, as well as detrital series (greywackes, pelites, conglomerates) metamorphosed in the greenschist to lower-amphibolite facies (Papon, 1973; Bessoles, 1977; Metelka *et al*., 2011).

The regional tectonic evolution is dominated by the Eburnean orogeny (2.2–2.0 Ga), articulated around several major deformation phases **(figure 1 B).** The D1 phase corresponds to an early event of thrusting and sub-horizontal structuring. The major D2 and D3 phases are characterized by transpressive tightening leading to the development of the regional S2 foliation, upright folds, and a vast network of transcurrent shear corridors, successively sinistral then dextral (Feybesse *et al*., 2006; Baratoux *et al*., 2011; Perrouty *et al*., 2012; Jessell *et al*., 2016).

At the scale of the Doropo district, the formations are crosscut by large brittle to ductile-brittle structures trending NNE–SSW to NE–SW. Recent aeromagnetic geophysical data confirm that the spatial distribution of gold occurrences is directly aligned with these major structural lineaments, which guided the hydrothermal drainage (Siagné *et al*., 2022).

3 MATERIALS AND METHODS

The methodological approach adopted is based on an integrated procedure combining field studies, laboratory analyses, and interpretation.

The fieldwork includes mapping and sample collection. This phase allows the gathering, listing, and plotting on a 1/50,000 base map of the artisanal mining zones, the points of the hydrographic network, the lowlands, the veins, the outcrops, and any geological information. The measurements were plotted on stereograms using the Georient software.

Quartz samples were collected in-situ from extraction pits, trenches, and surface outcrops. The structural orientations of the veins, foliation planes, and fractures were measured using a Suunto compass-clinometer.

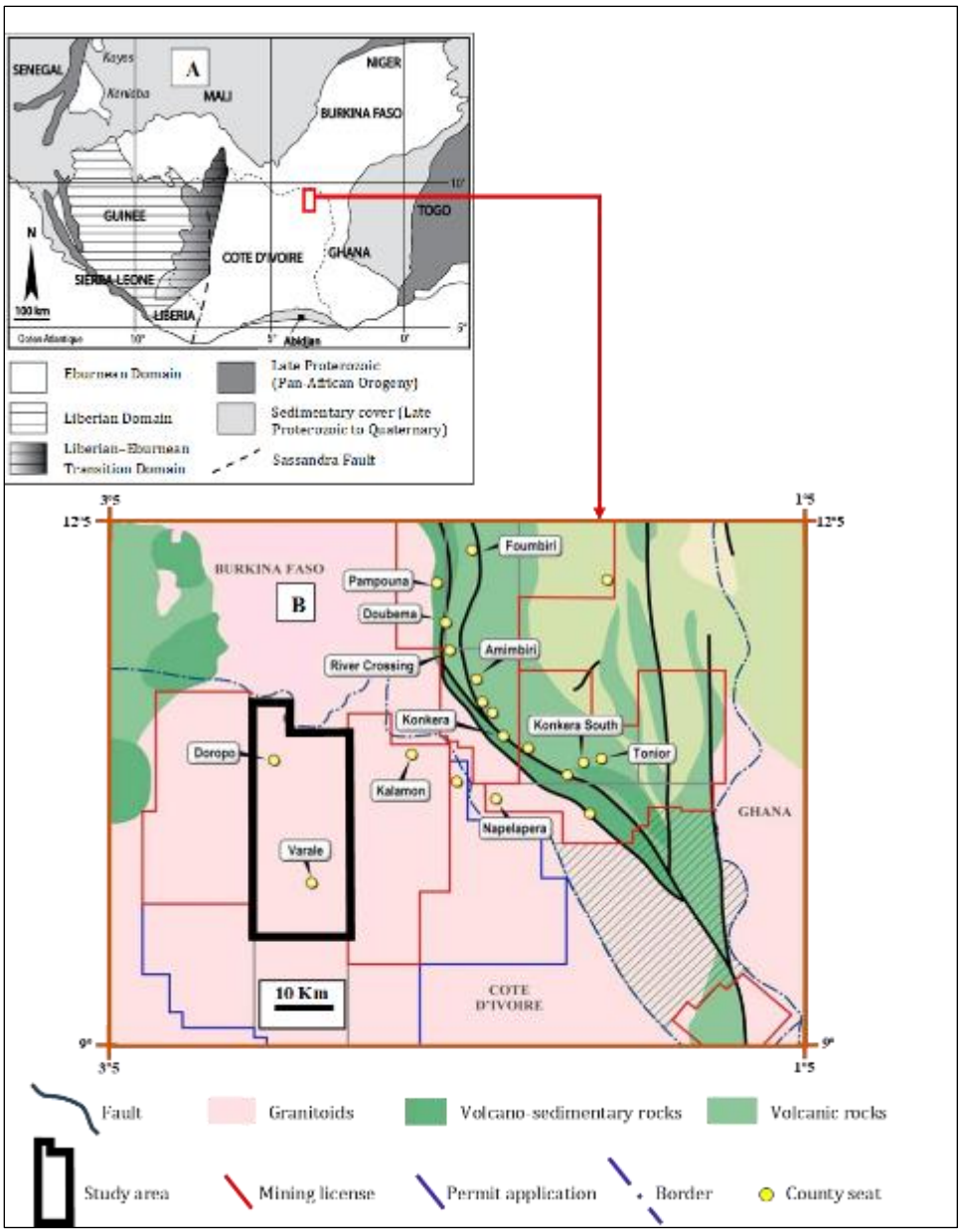


Figure 1: (A) Map of the Man ridge (Bessoles, 1977; modified); (B) Synthetic geological map of the Kalamon mining sector (CENTAMIN Report, 2017).

The petrographic and mineralogical study began with a macroscopic naked-eye description of the various quartz samples before proceeding with microscopic analysis under a polarizing microscope. The latter relied on the examination of about twenty thin sections, partly prepared at the University of Paris XI (France) and at the Centre for Analysis and Research (CAR) of the Société des Opérations Pétrolières de Côte d'Ivoire (PETROCI). All macroscopic and microscopic descriptions were carried out at the Laboratory of Geology, Mineral and Energy Resources of the UFR of Earth Sciences and Mineral Resources of Félix HOUPHOUET-BOIGNY University, Abidjan-Cocody. The metalliferous phase was studied in reflected light under a metallogenic microscope.

4 RESULTS

4.1 Petrographic typologies of quartz

The fieldwork makes it possible to divide the Doropo vein network into three quartz morphotypes with distinct characteristics:

4.1.1 Milky quartz veins

Macroscopically, the milky quartz veins occur as a massive habit, white to grey-whitish in color and locally translucent, with numerous fractures and small cavities (figure 2 A). Under the microscope, the quartz displays a coarse granoblastic texture with interlocked xenomorphic grains. Undulatory extinction is frequent and reflects deformation postdating crystallization. Numerous microfractures cut across the quartz grains. Accessory minerals include pyrite, iron oxides, and occasionally native gold (figure 2 B and C).

These veins probably correspond to the early phases of siliceous precipitation of the hydrothermal system.

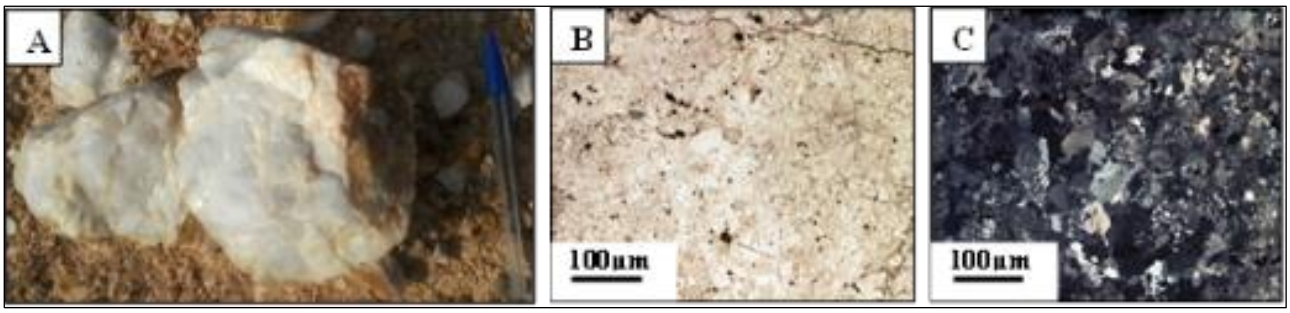


Figure 2: Macroscopic (A) and microscopic (B, C) appearance of the massive milky quartz collected at the artisanal extraction site of Doropo.

4.1.2 Smoky quartz veins

The smoky quartz veins display a dark color, grey-brown, light brown to dark brown (figure 3 A). This coloration is linked to the presence of carbonaceous inclusions, fine sulfide inclusions, or to natural radioactivity effects. It occurs as centimetric to metric veins injected into zones of intense shearing.

Under the microscope, smoky quartz shows granoblastic to subhedral textures with abundant microfractures and deformation lamellae. The original quartz grains (90%) display marked undulatory extinction, numerous deformation bands, strain lamellae, and a dense network of cataclased microfractures. Sulfides (brecciated xenomorphic pyrite, euhedral arsenopyrite) and iron oxides are frequently associated with these veins, as well as lithic or carbonaceous inclusions (figure. 3 B and C). Native gold is frequently identified as inclusions within the sulfides or trapped in the microfracture network.

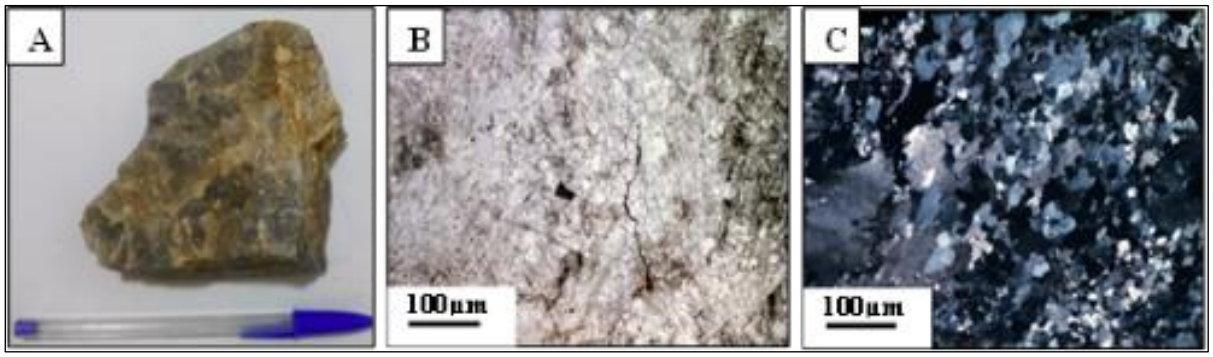


Figure 3: Smoky quartz sample showing a dark hue linked to the micro-particulate presence of sulfides and inclusions (A: macro; B, C: microscopy).

4.1.3 Saccharoidal quartz veins

Macroscopically, the saccharoidal quartz veins display a granular or “cane-sugar” texture made up of small bright crystals. Their color varies from white to light grey and yellow-orange (figure 4 A). Under the microscope, the texture is entirely fine to medium polygonal (equigranular granoblastic), composed of strongly interlocked xenomorphic (<80%) to subhedral quartz crystals displaying undulatory extinction (figure 4 B and C). It denotes intense dynamic recrystallization by grain-boundary migration or subgrain rotation. The crystals form a mosaic pattern with triple points at 120°. Accessory minerals include pyrite, iron oxides, and occasionally native gold.

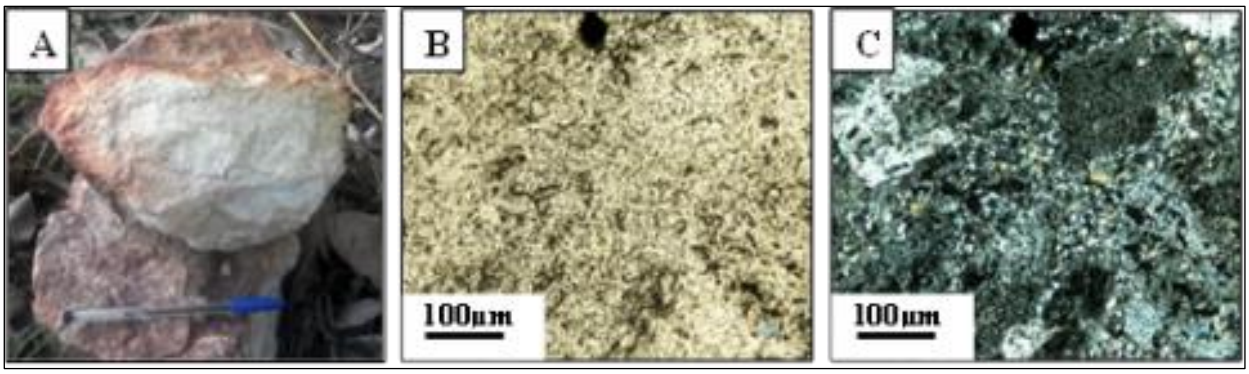


Figure 4: Friable saccharoidal quartz exposing an advanced granoblastic recrystallization texture (A: macro; B, C: microscopy).

4.2 Deformation

4.2.1 At the mesostructural scale

At the mesostructural scale, the quartz veins observed in the study area are distinguished by great geometric diversity, both in their thickness and in their orientations. Their thicknesses thus range from a few millimeters for the thinnest to several meters for the most imposing structures (figure 5 and 6). These vein networks, particularly predominant across the area, occupy a dense fracturing where the quartz crystals are frequently accompanied by secondary minerals such as calcite, chlorite, epidote, or hematite, witnesses of a polyphase hydrothermal circulation.

The statistical analysis of the structural data collected highlights three major orientation families (figure 7) that reflect the expression of a well-marked tectonic regime:

- A first family trending NW–SE, with steep dips inclined toward the SW (mean plane N132, 75°SW);
- A second family trending NE–SW, steeply upright toward the NW (mean plane N45, 85°NW);

Finally, a set of sub-meridian N–S veins, characterized by inclined dips (mean plane N5, 55°NW) (figure 5 A).

4.2.2 At the microstructural scale

At the microstructural scale, detailed examination of the quartz veins under the polarizing microscope reveals contrasting behavioral and deformational variations according to facies, reflecting a complex tectono-hydrothermal history.

Milky quartz is characterized by relatively moderate and poorly evolved intracrystalline deformation. The crystals most often retain sharp boundaries with weak to moderate undulatory extinction. This low substructuring is explained by its mode of occurrence: this quartz is mainly confined to the selvages of the vein structures, to fracture-margin zones, or to major lithological contacts between the granodioritic intrusions and the host dacites, where stresses were expressed in a more localized manner.

In contrast, smoky quartz records the imprint of particularly advanced intracrystalline deformation. It displays intense substructuring features, such as very marked banded undulatory extinction, subgrain development, and advanced polygonization, reflecting syn-tectonic recrystallization under high differential stresses. Moreover, the omnipresence of interconnected microfracture networks, extensional micro-fissures (micro-cataclasis), and ductile-brittle micro-shears generated a highly effective secondary permeability, conducive to the channeling and trapping of mineralizing hydrothermal fluids.

Finally, saccharoidal quartz shows a microgranular to sub-equigranular assemblage of small quartz crystals joined by right-angle or slightly lobate grain boundaries. This facies, which materializes late recrystallization phases or mechanically poorly evolved hydrothermal pulses, is distinguished by the absence or near-absence of open microfracture networks. This weak rheological response strongly restricted the possibilities of subsequent fluid percolation within this variety.



Figure 5: System of steeply dipping quartz veins (55 to 75°) in an artisanal mining pit.

4.2.3 On outcrop

In the field, the structural elements were difficult to measure due to the extent of meteoric alteration, which renders almost any outcrop invisible. Nevertheless, we were able to take a few measurements **(figure 6)** that confirm structures of the directional class [N120°–130°].

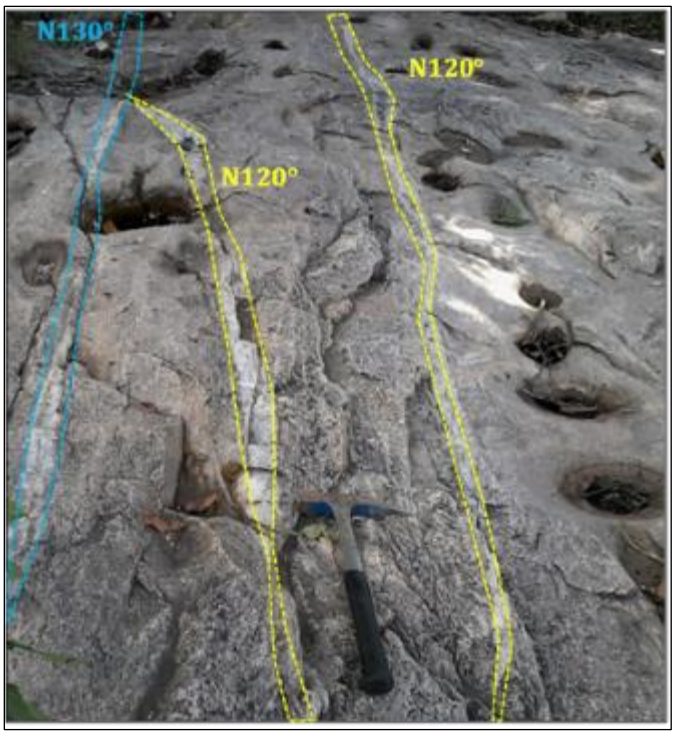


Figure 6: Photograph illustrating a granite outcrop with N 130° trending fractures filled with milky quartz.

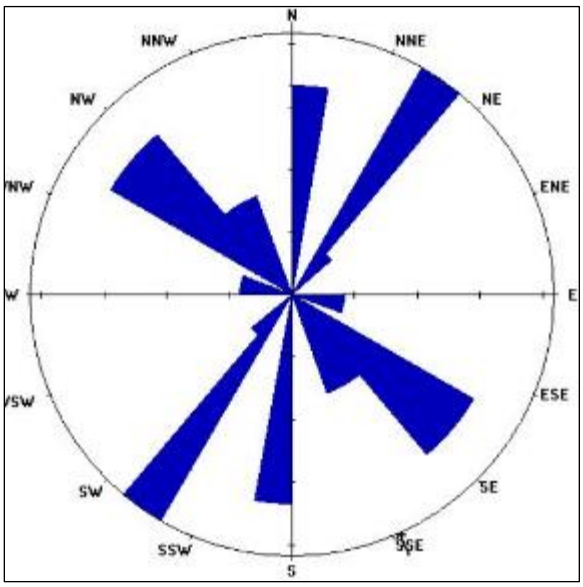


Figure 7: Directional rose diagram of the quartz veins and lodes in the Doropo artisanal mining sites, indicating the predominance of the NNE–SSW to NE–SW network.

4.3 Distribution of gold mineralization

The combined analysis of the petrographic and structural aspects of the quartz veins at Doropo, compared with the geochemical gold results and the field realities observed at the artisanal mining sites, highlights a clear metallogenic selectivity. Indeed, the quartz typology, its degree of microstructuring, and the abundance of associated sulfides prove to be valuable guides for understanding the distribution of native gold. Three main facies are thus distinguished:

First, smoky quartz asserts itself as the true driver of gold mineralization in the region. It concentrates the most remarkable grades, displaying an average of about 5 g/t Au. Gold appears there essentially in the free state, nestled within the syn- to late-hydrothermal microfractures crossing the crystals, or closely associated with sulfides (pyrite, arsenopyrite, and chalcopyrite). This demonstrates how much the reactivation of this quartz under a transpressive regime favored fluid circulation and gold precipitation **(figure 8).**

Next comes milky quartz, of a massive and macrocrystalline white, which visually represents the largest vein volume in the sector. Less generous, it displays low to moderate grades, around 3 g/t Au on average, which are generally confined to the selvages or contacts with the host rocks (granodiorites and dacites). As its internal deformation is much more subdued, gold is distributed there more erratically as rare disseminated grains, often accompanied by thin seams of chlorite and sericite **(figure 8).**

Finally, saccharoidal quartz, recognizable by its microgranular texture reminiscent of crystallized sugar, proves to be globally barren or very weakly mineralized. Its grades fluctuate around 1 g/t Au, or even below. Reflecting late recrystallization phases or poorly evolved hydrothermal inputs, this facies suffers from a lack of open microfracturing and a deficiency in primary sulfides, which offered it neither the permeability nor the geochemical trapping properties required for gold-bearing fluids **(figure 8).**

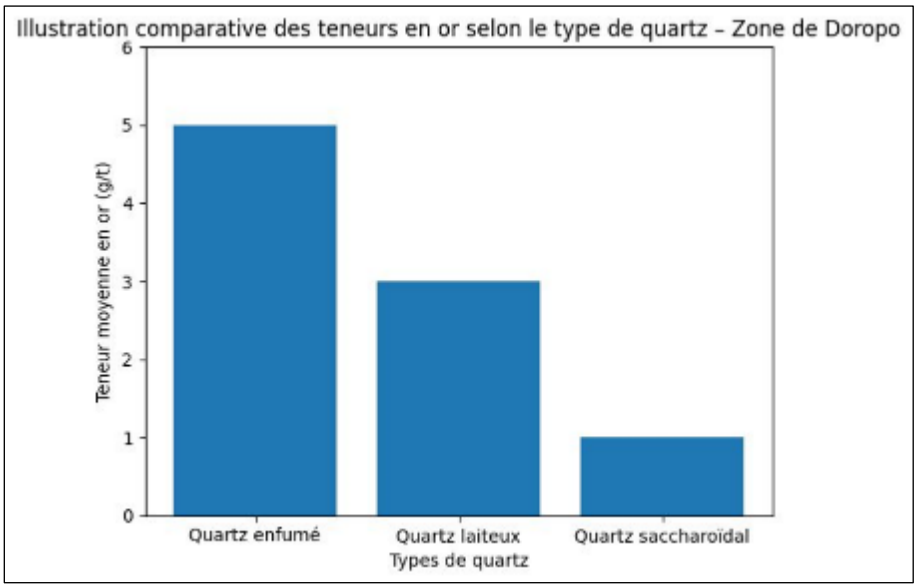


Figure 8: Average distribution of the recorded gold grades as a function of the quartz-vein typology in the Doropo zone.

5 DISCUSSION

5.1 Origin and evolution of hydrothermal fluids

The genesis of the quartz and gold systems of Doropo fits fully within the framework of the metamorphic dehydration of the Birimian volcano-sedimentary series during the Eburnean orogeny (Groves et al., 1998, 2018; Goldfarb et al., 2005, 2020). The deep fluids of hydro-carbonic and low-salinity composition (H_2O–CO_2–NaCl ± CH_4), carrying gold as bisulfide complexes (e.g., $Au(HS)_2^-$), were preferentially channeled along the shear corridors and crustal-scale weakness zones (Robert & Poulsen, 2001; Groves & Goldfarb, 2018). Fluid-pressure drops associated with episodic openings, coupled with fluid immiscibility reactions and chemical trapping by sulfidation at the wall-rock contact, triggered the destabilization of these complexes and the synchronous precipitation of smoky quartz, sulfides, and native gold.

5.2 Structural control and trapping of the mineralization

At the scale of the Doropo district, the major structural control is materialized by transcurrent strike-slip systems trending NNE–SSW to NE–SW (Siagné *et al*., 2022, 2025). The microstructural succession recorded by the different quartz facies reflects a continuous temporal and rheological evolution: it marks the transition from an early ductile regime responsible for the emplacement of the massive milky quartz in the selvage zones or at the lithological contacts, toward a ductile-brittle then strictly brittle regime (Sibson, 1990; Robert & Poulsen, 2001). This last stage is directly responsible for the development of smoky quartz, characterized by a dense network of cataclased microfractures.

The superimposition of cataclasis and dynamic recrystallization within smoky quartz acted as a highly effective secondary-permeability regulator, thereby maximizing the volumes of percolated hydrothermal fluids (Cox, 2005; Bons *et al*., 2012). The textures and deformation features observed in the field attest to a history of polyphase reopening (pump-action mechanism), marked by vein lenticularization, syn-hydrothermal brecciation, boudinage, and brittle re-fracturing (Sibson, 1990). Conversely, saccharoidal quartz, whose equigranular granoblastic texture testifies to late

injections or recrystallizations, remained impermeable in the absence of an open microfracture network, explaining its barren character.

5.3 Comparison with regional Birimian districts

The structural, petrographic, and metallogenic characteristics documented at Doropo show strong analogies with the orogenic gold-deposit models described at the scale of the West African Craton (Milési *et al*., 1989; Feybesse *et al*., 2006; Eglinger *et al*., 2017):

- In Ghana (Ashanti belt): an equivalent structural control is found through regional crustal fault structures, associated with quartz-carbonate-pyrite-arsenopyrite metamorphic parageneses where cataclased smoky quartz traps gold in extensional structures (Allibone *et al*., 2002; Lawrence *et al.*, 2013).
- In Mali and Burkina Faso: the Birimian gold districts show identical rheological behavior, where the microfractured smoky-quartz facies constitutes the main vector and trap of the precious metal, contrasting with the relative barrenness of the late milky or saccharoidal quartz phases (Lompo, 2009; Tarnagda *et al*., 2024; Royer & Camara, 2025).

6 CONCLUSION

In conclusion, the integrated study carried out on the Doropo sector highlights the decisive role of the coupling between petrographic and microstructural analysis and the typology of quartz veins in understanding the mechanisms of gold mineralization within the Paleoproterozoic of Côte d'Ivoire. The investigations made it possible to identify three distinct quartz morphotypes (milky, smoky, and saccharoidal), revealing a clear metallogenic selectivity:

- Smoky quartz, characterized by intense intracrystalline deformation, pronounced micro-cataclasis, and a close association with sulfides (pyrite, arsenopyrite), constitutes the main vector of highly concentrated gold (average of about 5 g/t Au).
- Milky quartz, associated with selvages and lithological contacts, displays more modest grades (~3 g/t Au).
- Saccharoidal quartz, resulting from late recrystallizations, remains globally barren or weakly mineralized (~1 g/t Au).

Structurally, the emplacement of these vein networks is closely controlled by shear corridors and brittle to ductile-brittle structures (with major NW–SE, NE–SW, and sub-meridian N–S families), reflecting a dynamic transition of tectonic regimes during the Eburnean orogeny. These results thus provide first-order exploration keys for the Doropo district and fit harmoniously within the regional metallogenic framework of the West African Craton, underlining the targeted importance of cataclased smoky-quartz structures for the optimization of future gold-prospecting programs.

STATEMENTS ON COMPLIANCE WITH ETHICAL STANDARDS

Acknowledgments

The authors would like to thank all those who contributed, directly or indirectly, to the writing of this paper.

Funding Source

Research grant awarded by Côte d'Ivoire.

Disclosure of conflict of interest

The authors declare no conflicts of interest regarding this manuscript.

REFERENCES

[1] Allibone, A., McCuaig, T. C., Harris, D., Etheridge, M., Munroe, S., Byrne, D., & Blenkinsop, J. (2002). Lower Proterozoic gold deposits in the Ashanti Belt, Ghana: Geochronological constraints. Economic Geology, 97(3), 505–517.

[2] Baratoux, L., Jessell, M. W., Feybesse, J. L., Ilboudo, H., & Cottereau, N. (2011). Initiation and paleoproterozoic accretion of the West African Craton. Precambrian Research, 187(3-4), 169–199.

[3] Bessoles, B. (1977). Géologie de l'Afrique : le Craton Ouest-Africain. Mémoires du BRGM, n° 88, Paris, 383 p.

[4] Block, S., Baratoux, L., Zeh, A., Eglinger, A., McFarlane, C. R., & Siebel, W. (2016). The Paleoproterozoic geologic history of the West African Craton in western Burkina Faso: An integration of U-Pb geochronology, Lu-Hf isotope systematics, and geochemistry. Precambrian Research, 274, 52–77.

[5] Bons, P. D., Koehn, D., & Jessell, M. W. (2012). Microfracturing and vein formation in geological systems. Springer Science & Business Media, 240 p.

[6] Cox, S. F. (2005). Coupling between deformation, fluid pressure variations, and fluid flow in fault-fracture meshes, with an example from the Ballarat goldfield, Victoria, Australia. Economic Geology, 100(1), 1–18.

[7] Eglinger, A., Bari, A., Robb, L. J., Augenstine, M., & Zeh, A. (2017). Paleoproterozoic crustal evolution and gold metallogeny of the West African Craton. Ore Geology Reviews, 81, 1050–1068.

[8] Feybesse, J. L., Billa, M., Guerrot, C., Duguey, E., Lescuyer, J. L., Milési, J. P., & Bouchot, V. (2006). The Paleoproterozoic of the West African Craton: A synthesis. Precambrian Research, 149(3-4), 127–154.

[9] Goldfarb, R. J., & Groves, D. I. (2015). Orogenic gold: Common or evolving fluid and metallogenic sources through time. Lithos, 233, 2–26.

[10] Goldfarb, R. J., Groves, D. I., & Gardoll, S. (2001). Orogenic gold and geologic time: A global synthesis. Ore Geology Reviews, 18(1-2), 1–75.

[11] Goldfarb, R. J., Baker, T., Dubé, B., Groves, D. I., Hart, C. J. R., & Gosselin, P. (2005). Distribution, character, and genesis of gold deposits in metamorphic terranes. Economic Geology 100th Anniversary Volume, 407–450.

[12] Goldfarb, R. J., Groves, D. I., & Santosh, M. (2020). Orogenic gold deposits: Celebrating 30 years of modern understanding. Geoscience Frontiers, 11(1), 1–9.

[13] Groves, D. I., & Goldfarb, R. J. (2018). Orogenic gold deposits: Past, present and future. Economic Geology, 113(1), 1–19.

[14] Groves, D. I., Goldfarb, R. J., Gebre-Mariam, M., Hagemann, S. G., & Robert, F. (1998). Orogenic gold deposits: A proposed classification in the context of their crustal distribution and relationship to other gold deposit types. Ore Geology Reviews, 13(1-5), 7–27.

[15] Groves, D. I., Goldfarb, R. J., Robert, F., & Hart, C. J. R. (2003). Gold deposits in metamorphic belts: Overview of current understanding, outstanding problems, future research. Economic Geology, 98(1), 1–29.

[16] Groves, D. I., Santosh, M., & Goldfarb, R. J. (2018). Structural and metamorphic controls on orogenic gold deposits. Geoscience Frontiers, 9(3), 633–645.

[17] Jessell, M. W., Baratoux, L., Sakho, Y., Amponsah, P. O., & Bourassa, Y. (2016). The geology of the West African Craton. Journal of African Earth Sciences, 121, 150–165.

[18] Kouamelan, A. N., Deloule, E., & Peucat, J. J. (2015). Geochronological evolution of the Paleoproterozoic in Côte d'Ivoire. Journal of African Earth Sciences, 105, 45–60.

[19] Lawrence, D. M., Simmons, S. F., & Seccombe, P. K. (2013). The epithermal-orogenic transition in Archaean/Paleoproterozoic gold deposits. Mineralium Deposita, 48(2), 185–201.

[20] Lompo, M. (2009). Geodynamic evolution of the Paleoproterozoic Birimian formations of the Liptako-Gourma region (Eastern Burkina Faso). Journal of African Earth Sciences, 53(1-2), 45–60.

[21] Metelka, V., Baratoux, L., Jessell, M. W., Gourgaud, A., & Naba, S. (2011). Geophysical imaging of the Paleoproterozoic Birimian formations of the West African Craton. Precambrian Research, 187(1-2), 45–66.

[22] Milési, J. P., Feybesse, J. L., Ledru, P., Dommanget, A., Marcoux, E., Egal, E., & Calvez, J. Y. (1989). Les minéralisations d'or du Birimien (Protérozoïque inférieur) de l'Afrique de l'Ouest. Ses relations avec l'évolution lithostructurale et géodynamique. Chronique de la Recherche Minière, 497, 3–58.

[23] Milési, J. P., Lescuyer, J. L., & Feybesse, J. L. (2004). Le Protérozoïque inférieur de l'Afrique de l'Ouest : une géodynamique exceptionnelle pour les minéralisations d'or. Comptes Rendus Geoscience, 336(4), 319–330.

[24] Papon, A. (1973). Géologie et minéralisations du Sud-Est de la Côte d'Ivoire. Mémoires du BRGM, n° 78, Paris, 240 p.

[25] Perrouty, S., Jessell, M. W., Baratoux, L., Bourassa, Y., & Miller, J. (2012). 3D structural model of the Ashanti belt, Ghana. Precambrian Research, 204-205, 116–135.

[26] Robert, F., & Poulsen, K. H. (2001). Vein formation and deformation in orogenic gold deposits. Reviews in Economic Geology, 14, 111–129.

[27] Royer, J., & Camara, M. (2025). Orogenic gold systems in Mali and Burkina Faso. Journal of African Earth Sciences, 202, 105120.

[28] Sibson, R. H. (1990). Faulting and fluid flow. Geological Society, London, Special Publications, 54(1), 69–84.

[29] Siagné, Z. H., Ouattara, A. S., Konan, N. J. J., & Kouamé, F. (2022). New Lithostructural Map of the Doropo Region, Northeast Côte d'Ivoire: Insight from Structural and Aeromagnetic Data. Journal of African Earth Sciences, 196, 104680.

[30] Siagné, Z. H., Ouattara, A. S., & Allou, Y. (2025). Integration of airborne gamma-ray spectrometry and remote sensing data for mapping of gold-bearing structures in the Doropo region, Northeastern Côte d'Ivoire. Geocarto International, 40(1), 2465074.

[31] Tarnagda, B., Naba, S., & Siele, I. (2024). Structural control of orogenic gold deposits in Burkina Faso. Journal of African Earth Sciences, 190, 104520.

[32] Vidal, M., & Alric, G. (1994). Geodynamic evolution of the Birimian of West Africa. Precambrian Research, 67(1-2), 115–130.

[33] Yao, B. J., Kouamé, F., & Tagini, B. (2016). Le domaine de Baoulé-Mossi en Côte d'Ivoire : Synthèse géologique. Journal des Sciences Géologiques, 14(1), 12–28.